Tie Lines of the Grain Boundary Wetting Phase Transition in the Al–Sn System

B. Straumal and W. Gust
Max-Planck-Institut für Metallforschung
and Institut für Metallkunde
Seestr. 75, D-70174 Stuttgart, Germany
and
D.Molodov
Institut für Metallkunde und Metallphysik
Kopernikusstr. 14, D-52074 Aachen, Germany

(Submitted March 10, 1994)

Temperature dependencies of contact angles θ at the intersection of grain boundaries in Al bicrystals with solid Al/liquid Al-Sn interphase boundaries were studied. For this purpose, two Al bicrystals were grown with tilt <011>{001} grain boundaries having misorientation angles φ = 38.5° (near Σ9 coincidence misorientation) and φ = 32°. These boundaries possess different energies. The temperatures T_w of the grain boundary wetting phase transition for these two boundaries were determined, and the corresponding conodes in the two-phase area of the Al-Sn phase diagram were constructed. Above T_w, the contact angle θ = 0 and a layer of the liquid phase completely wets the grain boundary. The temperature of wetting transition T_{w1} = 6047 ± 1 °C, for the grain boundary with high energy (φ = 32°) is lower than T_{w2} = 6177 ± 1 °C for the grain boundary with low energy (φ = 38.5°). Above the temperature interval where all the grain boundaries become wetted, the solid phase may exist only as isolated single crystalline "islands" in the "sea" of melted phase.

Introduction

Recently, tie lines depicting grain boundary (**GB**) phase transitions began to appear in bulk phase diagrams [92Str2, 91Rab1]. The addition of these equilibrium tie lines to bulk phase diagrams ensures adequate description of polycrystalline materials. In some cases, the complete phase diagrams showing GB tie lines assitst the interpretation of microstructure formation in various important technologies like liquid phase sintering [83Zov] or isothermal solidification [92Bar].

One of the most important GB phase transitions is the GB wetting transition. Consider the contact between a bicrystal and a liquid phase L (Fig. 1). If the GB energy σ_{GB} is lower than $2\sigma_{SL}$ (σ_{SL} is the energy of solid-liquid interface), the GB is not wetted and the contact angle $\theta > 0$ (Fig. 1a). If $\sigma_{GB} > 2\sigma_{SL}$, the GB is wetted by the liquid phase and $\theta = 0$ (Fig. 1b). If the temperature dependencies $\sigma_{GB}(T)$ and $2\sigma_{SL}(T)$ intersect, then the GB wetting phase transition proceeds at the temperature T_w of their intersection (Fig. 1c). The contact angle θ decreases gradually with increasing temperature to zero at T_w (Fig. 1d). At $T > T_w$, the contact angle θ = 0. The conode (tie line) of the GB wetting phase transition appears at T_w in the two-phase region (S+L) of the bulk phase diagram. Above this conode, GBs with an energy σ_{GB} cannot exist in equilibrium with the liquid phase. The liquid phase forms a layer separating the crystals. The decreasing of the contact angle θ to 0 at T_w was first observed in polycrystalline samples: Zn-Sn [77Pas], Al-Sn [49Ike, 63Rog], Al-Cd [63Rog], Al-In [63Rog], Al-Pb [49Ike], and Ag-Pb [82Pas]. In later measurements, bicrystals with individual GBs were also used: (Fe-Si)-Sn [91Rab2], (Fe-Si)-Zn [91Nos, 91Rab2], and Cu-In [92Str2].

If two GBs have different energies, σ_{GB1} and σ_{GB2}, the temperatures of GB wetting transitions T_{w1} and T_{w2} will also differ—the lower σ_{GB}, the higher T_w (Fig. 1d). Therefore, there is a family of GB wetting transition conodes in the two-phase region (S+L) of the bulk phase diagram that correspond to GBs with different energies. The experiments show that this difference is not negligible. For example, the difference between T_w for GBs in Cu bicrystals in contact with an In-rich melt is ~30 °C [92Str2]. Therefore, it is not correct to measure T_w in polycrystals. For the construction of GB wetting transition conodes in the bulk phase diagram, bicrystals with GBs having different σ_{GB} values must be used.

The information about GB wetting phase transitions is important not only for two-phase alloys. In homogeneous solid solutions, other GB phase transitions can take place [88Die, 91Rab1], which can essentially alter the GB properties [90Rab, 91Rab2, 91Nos, 92Str1] and therefore those of polycrystals. The lines of GB phase transitions like prewetting or premelting must begin at the end of the conode of the GB wetting transition on the solidus line [88Die, 91Nos].

The goal of this work was to construct experimentally the GB wetting conodes in the Al-Sn system in the field where solid Al and Sn-rich melt coexist. The investigation of GB phase transition lines in Al-based binary systems is driven by the extraor-

dinary technological importance of Al alloys. The experiments with polycrystalline samples show that there is a GB wetting phase transition in the Al-Sn system between 580 and 620 °C [63Rog]. In the present studies, measurements have been made for individual GBs having different energies.

Experimental

Selection of GB Misorientation Parameters and Bicrystal Growth

There is experimental evidence that GB wetting phase transitions proceed in the Al-Sn system, but the temperature T_w was measured on polycrystalline samples and was not determined exactly enough [63Bor]. As stated above, it is not correct to define the conodes of the GB wetting transition in the bulk phase diagram using two-phase polycrystals due to the difference between T_w for GBs with different energies. It would be very important to determine the minimal T_w, which must correspond to the GB with highest possible energy. Unfortunately, the published experimental data about GB energies do not allow us to define without doubt the crystallographic parameters of such a GB. The other way is to determine the temperature interval where the wetting phase transition will occur for most GBs with different energies.

In order to estimate the temperature interval of T_w for GBs with different energies σ_{GB}, we decided to choose one GB with high energy σ_{GB1} and one GB with low energy σ_{GB2}. It is known that the "special" GBs having misorientation angles φ lying close enough to the coincidence misorientations with low Σ (Σ being the reciprocal density of coincidence sites) possess a low energy [85Str]. The GBs with misorientations far from the coincidence (beyond the regions of existence of "special" GBs) have high energy. Using the data of experiments and computer modelling of relative energies of tilt <011>{001} GBs in Al [71Has], we have selected two symmetrical tilt <011>{001} GBs: one with low energy and misorientation angle φ lying near the $\Sigma 9$ coincidence misorientation of 38.94° and one with high energy and $\varphi = 32°$ far from $\Sigma 9$ coincidence misorientation (beyond the region of existence for $\Sigma 9$ "special" GBs [85Str]). The energies of these GBs are different by about 30% [71Has]. In the interval between σ_{GB1} and σ_{GB2} lie the σ_{GB} values for most GBs. Therefore, the temperatures of wetting transition T_w for most GBs must also lie between T_{w1} and T_{w2} for the GBs selected.

The bicrystals were produced from Al of 99.999 wt.% purity using the directed crystallization method, which allows growth of the bicrystals with all possible crystallographic parameters of GBs [78Ale]. At intermediate stages of bicrystal production, the monocrystal seeds were etched for 1 to 5 min in a solution of 10 ml HF, 50 ml HNO_3, and 50 ml HCl and oriented directly on the spark erosion machine by a laser optical method [84Pro]. Finally, the orientation of the crystallographic axes of the bicrystals was controlled using Laue back reflection. The misorientations of grains in bicrystals were also defined by measuring of misorientations of etching pits on the surface of both grains using an optical microscope. For this purpose, the samples were etched in a solution of 90 ml HCl, 45 ml HNO_3, and 10 ml HF. The flat bicrystals, having dimensions 2 × 8 × 120 mm with the flat GB lying parallel to the long axis and perpendicular to the (011) surface, were grown in high-purity graphite crucibles in an atmosphere of high-purity argon (with oxygen concentration equivalent to a vacuum of 10^{-5} Pa). Two bicrystals

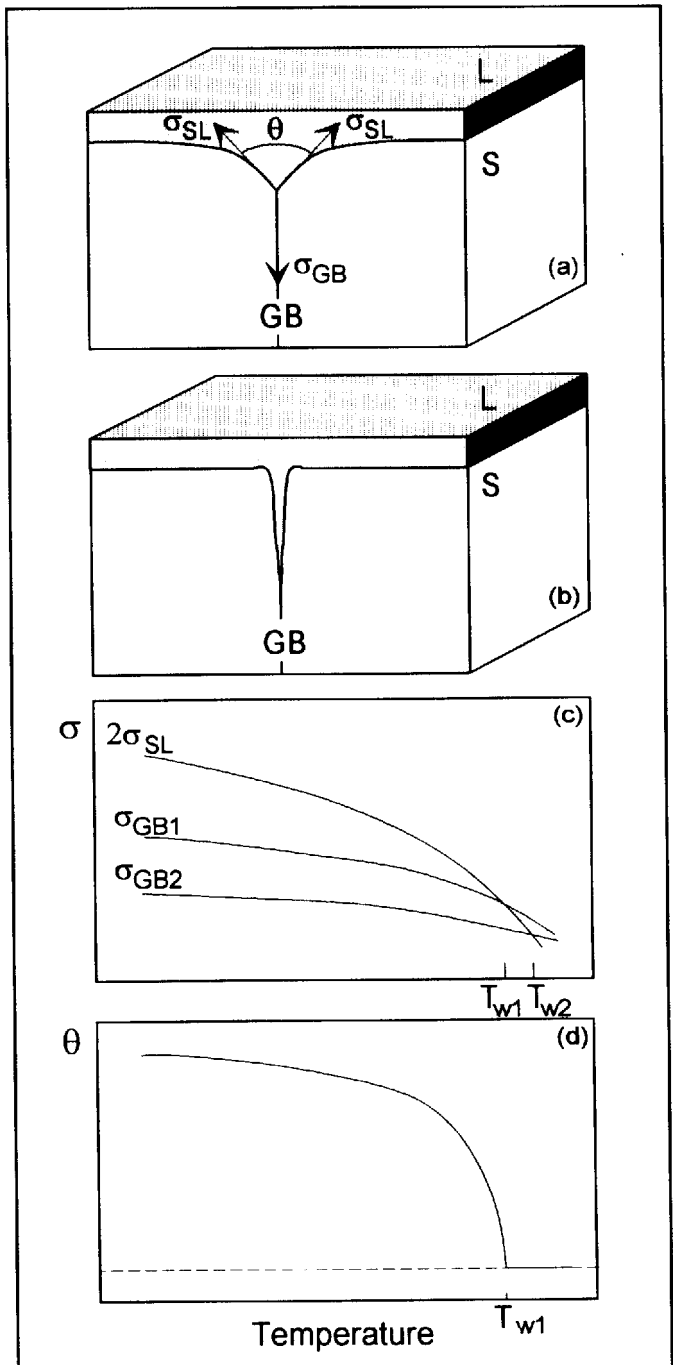

Fig. 1 (**a**) Bicrystal in contact with a liquid phase. GB is not wetted: θ>0. (**b**) GB is wetted: θ=0. (**c**) Schematic temperature dependencies of GB energy $\sigma_{GB}(T)$ and energy of two solid/liquid interphase boundaries $2\sigma_{SL}(T)$. They intersect at temperatures T_{w1} and T_{w2} of GB wetting phase transition. (**d**) Schematic temperature dependency of contact angle θ corresponding to the scheme in Fig. 1c.

with tilt <011>{001} GBs having misorientation angles φ = 38.5 ± 0.5° (near Σ9 coincidence misorientation) and φ = 32 ± 1° were produced. After growing, the bicrystals were cut by spark erosion as 40-mm long pieces.

Wetting Experiments

For wetting experiments, samples with a Sn layer were then produced (Fig. 2). For this purpose, the Al bicrystals were etched for 40 to 60 s with the solution mentioned above and brought in contact with liquid Sn of 99.9999 wt.% purity at ~240 °C in an apparatus made from high-purity graphite (Fig. 2). The surface layer at the end of the Al bicrystal dissolves in liquid Sn and saturates the melt up to liquidus concentration at 240 °C. The contact between melted Sn(Al) and the Al bicrystal forms within a few seconds. Then the apparatus was cooled, and the Sn-coated Al sample was cut by spark erosion. The samples were 2 to 3 mm long with 0.2 to 0.4 mm thick Sn layers (Fig. 2b). The ratios between length of Al bicrystal and thickness of Sn-rich layer were selected so that the average sample composition during the subsequent anneal was in the two-phase field of the Al-Sn phase diagram [90Mas].

The Al bicrystals coated with a Sn-rich layer were then placed in evacuated silica ampoules with a residual pressure of approximately 4×10^{-4} Pa together with an oxygen getter (a piece of Ta foil). The samples were then annealed for 20 min at various temperatures between 357 and 625 °C and subsequently water quenched. The temperature in the sample reached the temperature of the furnace within approximately 10 min. For another 10 min, the sample was annealed at the prescribed temperature, which was maintained constant within ± 0.3 °C. Af-

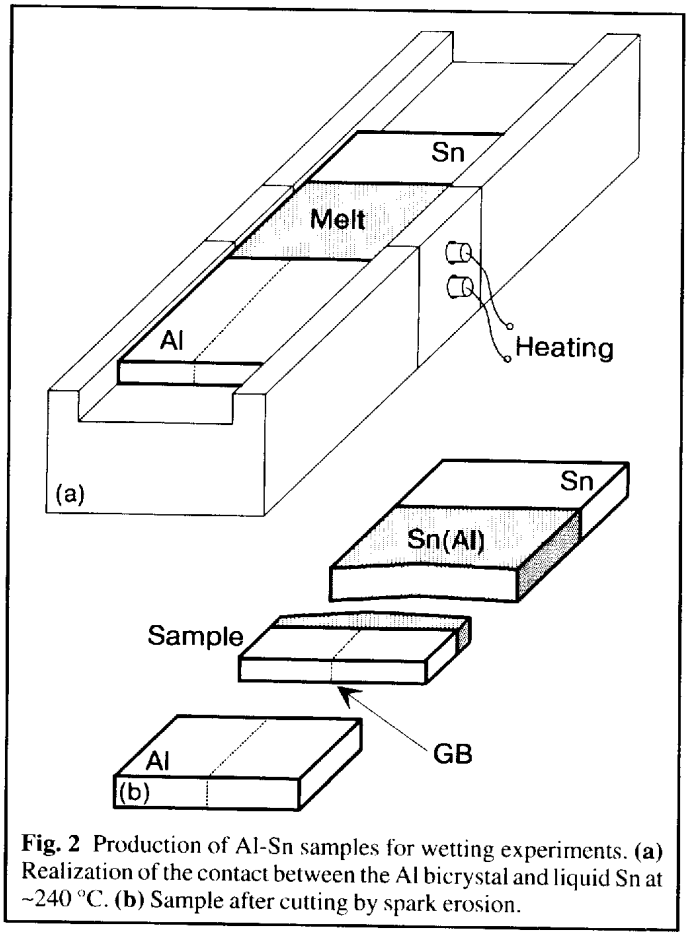

Fig. 2 Production of Al-Sn samples for wetting experiments. **(a)** Realization of the contact between the Al bicrystal and liquid Sn at ~240 °C. **(b)** Sample after cutting by spark erosion.

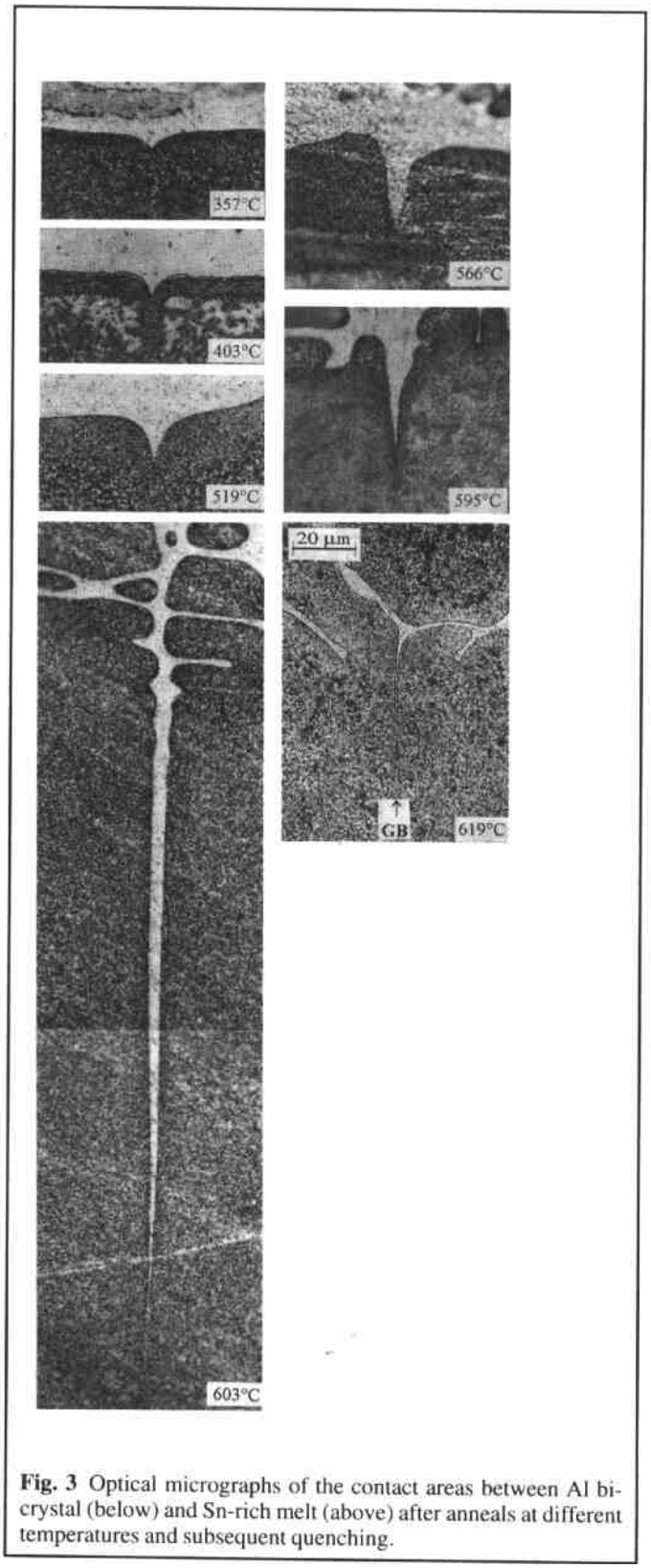

Fig. 3 Optical micrographs of the contact areas between Al bicrystal (below) and Sn-rich melt (above) after anneals at different temperatures and subsequent quenching.

ter quenching, the samples were embedded in a holder with Wood's metal and then mechanically ground and polished to make a polished surface parallel to the (001) surface of the Al bicrystal and perpendicular to the GB and solid/liquid interface. The polished surface was etched in a 5% aqueous solution of HF for a few seconds. The contact area between GB and interphase boundary was photographed in an optical microscope at a magnification of 1000×, and the contact angle θ was measured.

Results

Figure 3 shows the optical micrographs of the 32° <011>{001} GB for different temperatures. The advantage of the Al-Sn system in comparison with the Cu-In system [92Str2] is that the solubility of Sn in solid Al is very low and the liquidus concentrations in the temperature interval studied are high. Therefore, the position of the former liquid/solid interface can be easily evaluated after etching without searching for the position of the concentration step with aid of microprobe analysis. Only at high temperatures, above T_w, is the metallographic contrast poor, but it is still much better than in the Cu-In system [92Str2]. The GB lies perpendicular to the plane of Al-Sn contact and to the sample surface (section surface). This makes the measurement of the contact angle θ easier in comparison with experiments on polycrystals where the droplets of liquid phase are distributed randomly. The GBs are inclined to the section surface, and the angles measured on this section do not give the true dihedral angles. As shown in Fig. 3, the contact angle θ decreases with temperature T, tends to zero at $T=T_w$, and remains zero at $T>T_w$.

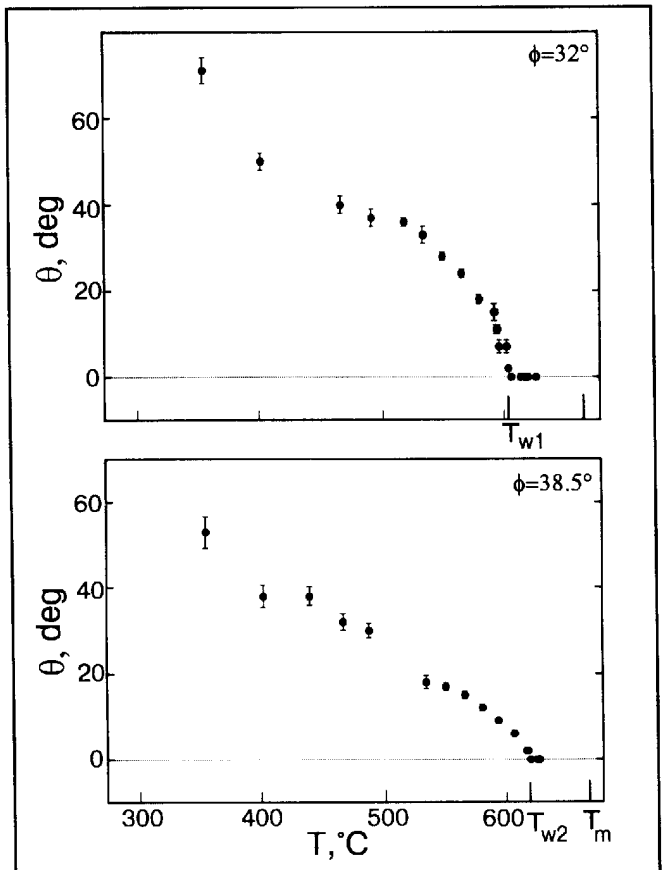

Fig. 4 Temperature dependencies of contact angle θ for 38.5° <011>{001} and 32° <011>{001} GBs. The wetting temperatures T_{w1} and T_{w2} are 604 and 617 ± 1 °C, respectively.

The temperature dependencies of the contact angles of both GBs studied are shown in Fig. 4. These data are also given in Table 1. The contact angle θ decreases in both cases with increasing temperature. At all temperatures below T_{w1}, the contact angles for the GB with φ = 38.5° lie lower in comparison with θ for the GB with φ = 32°. This means the energy σ_{GB2} is lower than σ_{GB1} as was supposed by selection of the GB misorientation parameters.

At the temperature T_w, the GB wetting phase transition happens. At $T>T_w$ the contact angle θ = 0. Both GBs studied have different temperatures of wetting phase transition: T_{w1} = 604 ± 1 °C for the 32° <011>{001} GB with high energy and T_{w2} = 617 ± 1 °C for the 38.5° <011>{001} GB with low energy.

Figure 5 shows the Al-Sn bulk phase diagram along with the conodes T_{w1} and T_{w2} of the GB wetting transition for the GBs studied. The borders of bulk phase fields are represented by thick lines and the GB wetting conodes by thin lines.

Discussion

The conodes of GB wetting transition lie in the temperature interval where the solubility of Sn in the liquid phase decreases very fast. In systems like Zn-Sn [77Pas] or Al-Cd [63Rog], the GB wetting temperatures coincide with temperatures where

Table 1 Contact Angles θ for the GBs with φ=32° and φ=38.5°

Temperature, °C	θ, degree (φ=32°)	θ, degree (φ=38.5°)
357 ± 0.3	71 ± 3	53 ± 2
403.3 ± 0.3	50 ± 2	38 ± 1
440.5 ± 0.3	...	38 ± 1
467.9 ± 0.3	40 ± 2	32 ± 3
488.5 ± 0.3	...	30 ± 2
493 ± 0.3	37 ± 2	...
519.4 ± 0.3	36 ± 1	...
534.5 ± 0.3	33 ± 2	18 ± 2
550.2 ± 0.3	28 ± 1	17 ± 2
565.5 ± 0.3	24 ± 1	15 ± 2
579.5 ± 0.3	18 ± 1	12 ± 1
591.3 ± 0.3	15 ± 2	...
592.4 ± 0.3	15 ± 2	9 ± 1
593.6 ± 0.3	11 ± 1	...
594.5 ± 0.3	11 ± 1	...
596.7 ± 0.3	7 ± 1.5	...
601.7 ± 0.3	7 ± 1.5	...
603.1 ± 0.3	2 ± 0.5	...
605.3 ± 0.3	0	6 ± 1
612.7 ± 0.3	0	...
614.8 ± 0.3	...	2 ± 1
616.3 ± 0.3	0	2 ± 1
618.2 ± 0.3	...	0
618.9 ± 0.3	0	...
623.5 ± 0.3	...	0
625.3 · 0.3	0	0

the liquidus line has a low concentration slope. This is not surprising because in this case the difference between liquidus and solidus concentrations decreases very fast with increasing temperature. The same is true for the surface tension of the solid/liquid interface σ_{SL}. Therefore, it is possible that $2\sigma_{SL}$ will be lower than σ_{GB} above a certain temperature.

The temperatures of GB wetting phase transitions determined here for two different GBs agree with experiments on polycrystals where the contact angle θ (averaged for 100 to 200 GBs) had a value of $\theta = 25°$ at 580 °C and $\theta = 0°$ at 620 °C [63Rog]. Using the published data [71Has], we chose the individual GBs so that the energy of most other GBs in Al lie between σ_{GB1} and σ_{GB2}. Therefore, the values of T_w for most Al GBs wetted by Sn(Al) melt lie between $T_{w1} = 604$ °C and $T_{w2} = 617$ °C. We see that T_{w2} (being the wetting transition temperature for the GB with the lower energy) really coincides with the temperature where most GBs in a polycrystal are wetted by a Sn-rich melt [63Rog].

Our data permit the estimation of the minimal temperature T_{wmin} at which the GBs with the highest energy begin to be wetted. Consider the scheme in Fig. 1e. The line $\sigma_{GBmax}(T)$ for the GB with highest energy lies higher in comparison with $\sigma_{GB1}(T)$ and $\sigma_{GB2}(T)$. Suppose that the $\sigma_{GB}(T)$ and $\sigma_{SL}(T)$ dependencies are linear near T_{w1} and T_{w2}. Calculations and measurements show that the ratio $\sigma_{GBmax}/\sigma_{GB1}$ is about 1.6 times higher than $\sigma_{GB1}/\sigma_{GB2}$ [71Has]. The linear extrapolation gives us a rough estimation for the minimal T_w value: $T_{wmin} = 582 \pm 5$ °C. Therefore, at a temperature of 580 °C where the averaged contact angle was $\theta = 25°$ [63Bor], no wetted GBs exist in a polycrystal.

Figure 6 shows a schematic bulk phase diagram with lines of GB wetting phase transition. The most important feature of the GB phase transition is that below T_w the GBs can exist in equilibrium with the melt. Above T_w conversely, the same GBs cannot exist in contact with a melt having the equilibrium liquidus concentration. The melt will penetrate along the GBs. Of course, this penetration process has its own kinetics and needs a distinct time. Therefore, the liquid layer in Fig. 3 is penetrated along the GB only at 40 to 50 μm after 10 min annealing.

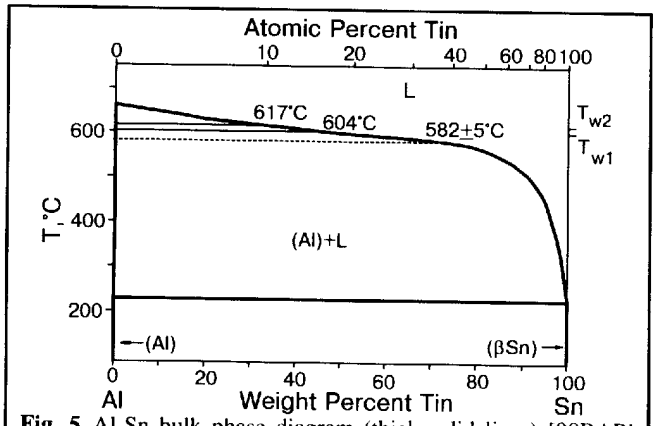

Fig. 5 Al-Sn bulk phase diagram (thick solid lines) [90BAP] along with the conodes of GB wetting transition (thin solid lines) at $T_{w1} = 604 \pm 1$ °C for the tilt 32°<011>{001} GB and at $T_{w2} = 617 \pm 1$ °C for the tilt 38.5°<011>{001} GB. The extrapolated minimal possible temperature of GB wetting phase transition $T_{wmin} = 582 \pm 5$ °C for the GBs with maximal energy is also shown (dotted line).

In Fig. 6, three lines of GB wetting phase transitions are schematically shown analogous to Fig. 5. The microstructures of two-phase polycrystals are also schematically shown for four different temperature intervals. Below T_{wmin}, all contact angles $\theta > 0$, and the liquid phase has the form of isolated droplets. Above T_{wmin}, and between lines of wetting phase transition for other GBs, some GBs are wetted, and others are not wetted. Above T_{w2}, most GBs are wetted, and the solid phase may exist only as isolated single crystalline "islands" in the "sea" of melted phase. In principle, for GBs with very low energy (twin GBs, low angle GBs) there is no T_w if $2\sigma_{SL} > \sigma_{GB}$ at T_m where T_m is the melting temperature. In such cases an incomplete wetting of the GB will occur at T_m.

According to [85Pas], some additional information can be extracted from the temperature dependencies $\theta(T)$. In our case the dependencies $\theta(T)$ for both GBs studied decrease monotonically with negative curvature, as temperature is increased, and drops to zero at a temperature below the liquidus. Therefore, in our case analogous to the Zn-Sn system analyzed in [85Pas], the first temperature derivatives $\partial\sigma_{GB}/\partial T$ and $\partial\sigma_{SL}/\partial T$ remain negative at all temperatures studied. It corresponds to the scheme drawn by us in Fig. 1e.

At a fixed temperature, the condition of force equilibrium at the triple point is:

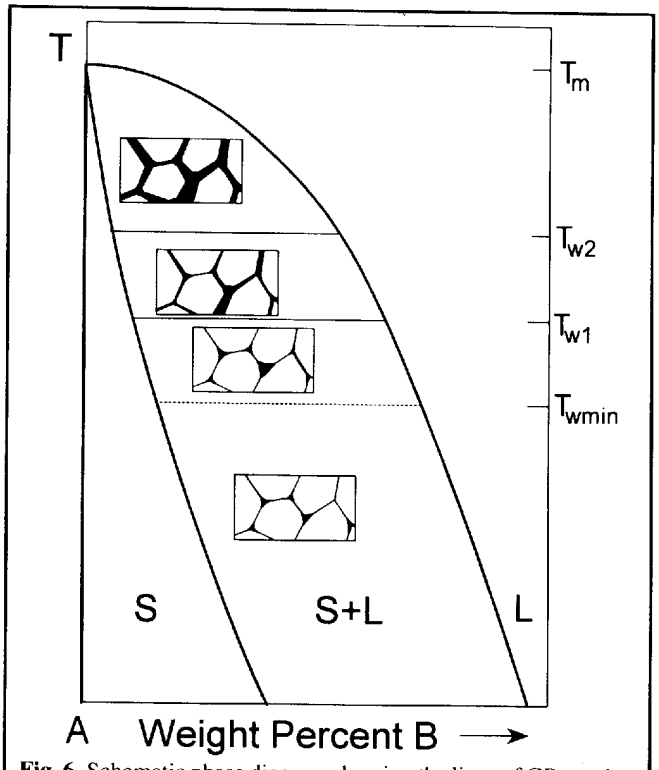

Fig. 6 Schematic phase diagram showing the lines of GB wetting phase transitions and the corresponding microstructures of two-phase polycrystals.

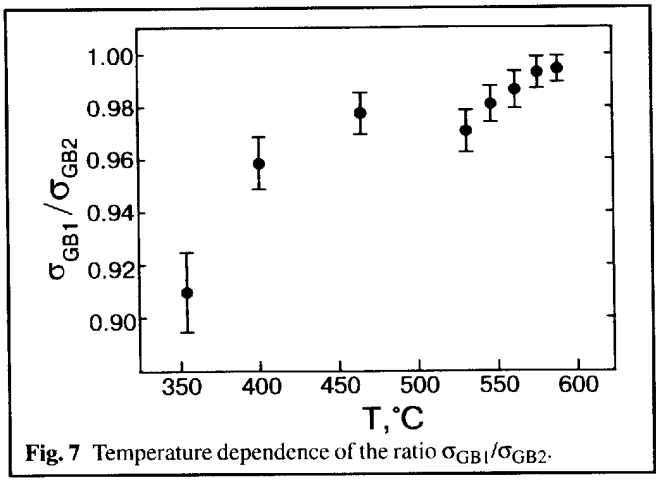

Fig. 7 Temperature dependence of the ratio $\sigma_{GB1}/\sigma_{GB2}$.

$\sigma_{GB} = \sigma_{SL} \cos(\theta/2)$.

Therefore, if we suppose that the energy of the solid/liquid interface σ_{SL} does not depend on its orientation relative to the crystal lattice of Al, we can estimate the temperature dependence of the ratio $\sigma_{GB1}/\sigma_{GB2}$:

$$\frac{\sigma_{GB1}}{\sigma_{GB2}} = \frac{\cos(\theta_1/2)}{\cos(\theta_2/2)}$$

This temperature dependence is shown in Fig. 7. It can be seen that σ_{GB2} is lower than σ_{GB1} as mentioned above. The ratio $\sigma_{GB1}/\sigma_{GB2}$ tends to 1 with increasing temperature. This means that the difference between σ_{GB1} and σ_{GB2} diminishes with increasing temperature (Fig. 1e).

Acknowledgments

The authors are grateful to Professors Brèchet, Gottstein, and Shvindlerman and Dr. Chenal and Dr. Rabkin for fruitful discussions. One of us (D.M.) wishes to thank the Alexander-von-Humboldt Foundation for the financial support.

Cited References

49Ike: K.K. Ikeuye and C.S. Smith, "Studies of Interface Energies in Some Aluminium and Copper Alloys," *Trans. Am. Inst. Met. Engrs*, *185*, 762-768 (1949).

63Rog: J.H. Rogerson and J.C. Borland, "Effect of the Shapes of Intergranular Liquid on the Hot Cracking of Welds and Castings," *Trans. Am. Inst. Met. Engrs*, *227*, 2–7 (1963).

71Has: G.C. Hasson and C. Goux, "Interfacial Energies of Tilt Boundaries in Aluminium. Experimental and Theoretical Determination," *Scr. Metall.*, *5*, 889-894 (1971).

77Pas: A. Passerone, N. Eustathopoulos, and P. Desrè, "Interfacial Tensions in Zn, Zn-Sn and Zn-Sn-Pb Systems" *J. Less-Common Met.*, *52*, 37–49 (1977).

78Ale: A.N. Aleshin, V.Yu. Aristov, B.S. Bokstein, and L.S. Shvindlerman, "Kinetic Properties of <111> Tilt Boundaries in Aluminium," *Phys. Status Solidi. (a)*, *45*, 359–366 (1978).

82Pas: A. Passerone, R. Sangiorgi, and N. Eustathopuolos, "Interfacial Tensions and Adsorbtion in the Ag–Pb System," *Scr. Metall.*, *16*, 547-550 (1982).

83Zov: P.E. Zovas, R.M. German, K.S. Hwang and C.J. Li, "Activated and Liquid Phase Sintering—Progress and Problems," *J. Met.*, *35*, 28–33 (1983).

84Pro: S.I. Prokofiev, B.B. Straumal, and I.N. Sorin, "Express-orientation and Precision Cutting of Crystals with Aid of Optical Orientation Method," *Ind. Lab.*, *50*, 45-46 (1984) in Russian.

85Pas: A. Passerone and R. Sangiorgi, "Solid-solid Interfacial Tensions by the Dihedral Angle Method. A Mathematical Approach," *Acta Metall.*, *33*, 771–776 (1985).

85Str: B.B. Straumal and L.S. Shvindlerman, "Regions of Existence of Special and Non-Special Grain Boundaries," *Acta Metall.*, *33*, 1735-1749 (1985).

88Die: S. Dietrich, "Wetting Phenomena," *Phase Transitions and Critical Phenomena*, *12*, Academic Press, New York, 1-218 (1988).

90Mas: *Binary Alloy Phase Diagrams*, T.B. Massalski, P.R. Subramanian, H. Okamoto, and L. Kacprzak, Ed., Vol 1, ASM International, Materials Park, OH, 216 (1990).

90Rab: E.I. Rabkin, L.S. Shvindlerman, and B.B. Straumal, "Diffusion of Indium Along <001> Sn-Ge Interphase Boundaries: Prewetting Phase Transition and Critical Phenomena," *J. Less-Common Met.*, *159*, 43-52 (1990).

91Nos: O.I. Noskovich, E.I. Rabkin, V.N. Semenov, B.B. Straumal, and L.S. Shvindlerman, "Wetting and Premelting Phase Transitions in 38°<100> Tilt Grain Boundaries in (Fe-12at.%Si)-Zn Alloy in the Vicinity of the A2-B2 Bulk Ordering in Fe-12at.%Si Alloy," *Acta Metall. Mater.*, *39*, 3091-3098 (1991).

91Rab1: E.I. Rabkin, L.S. Shvindlerman, and B.B. Straumal, "Grain Boundaries: Phase Transitions and Critical Phenomena," *Int. J. Mod. Phys.*, *B5*, 2989-3028 (1991).

91Rab2: E.I. Rabkin, V.N. Semenov, L.S. Shvindlerman, and B.B. Straumal, "Penetration of Tin and Zinc Along Tilt Grain Boundaries 43°<100> in Fe-5at.%Si Alloy: Premelting Phase Transition?" *Acta Metall. Mater.*, *39*, 627-639 (1991).

92Bar: F. Bartels, T. Muschik, and W. Gust, "Investigation on Thermally Stable Microjoints Consisting of Intermetallic Phases," *DVS-Berichte*, *141*, 22-24 (1992) in German.

92Str1: B.B. Straumal, O.I. Noskovich, V.N. Semenov, L.S. Shvindlerman, W. Gust, and B. Predel, "Premelting Transition on 38°<100> Tilt Grain Boundaries in (Fe-10at.%Si)-Zn Alloys," *Acta Metall. Mater.*, *40*, 795-801 (1992).

92Str2: B. Straumal, T. Muschik, W. Gust, and B. Predel, "The Wetting Transition in High and Low Energy Grain Boundaries in the Cu(In) System," *Acta Metall.Mater.*, *40*, 939-945 (1992).